AAPS PharmSciTech (2022) 23: 80
DOI: 10.1208/s12249-022-02223-x

Research Article

Theme: Advancements in Amorphous Solid Dispersions to Improve Biavailabilty

An Insight into Eudragit S100 Preserving Mechanism of Cinnarizine Supersaturation

Maryam Maghsoodi,[1,7] Saeideh Mollaie Astemal,[2] Ali Nokhodchi,[3] Hossein Kiaie,[4,5] Ali Baradar Khoshfetrat,[2] and Fatemeh Talebi[6]

Received 23 October 2021; accepted 17 January 2022 ; published online 1 March 2022

Abstract. Generally, supersaturation of weakly basic drug solution in the gastrointestinal tract can be followed by precipitation, and this can compromise the bioavailability of drugs. The purpose of this study was to evaluate the effect of Eudragit® S100 on the pH-induced supersaturation of cinnarizine and to examine the preserving mechanism of cinnarizine supersaturation by Eudragit®. Variables, including pH of media, ionic strength, and degree of supersaturation, were studied to investigate the effects of these parameters on cinnarizine supersaturation in the presence and absence of Eudragit®. The size of the Eudragit® aggregate in solution using dynamic light scattering was determined. The effect of Eudragit® on the transport of cinnarizine through the Caco-2 membrane was also investigated. The particle size study of Eudragit® aggregates showed that the size of these aggregates become large when the pH was lowered. Supersaturation experiments also demonstrated that Eudragit® preserved higher cinnarizine supersaturation with increasing ionic strength of the solution. The phase separation behavior of cinnarizine solution as a function of the degree of the supersaturation could be readily explained by considering the drug amorphous solubility. *In vitro* permeation studies revealed that the rate of cinnarizine permeation across Caco-2 cells increased in the presence of Eudragit®. According to the obtained results, the aggregation status of Eudragit® and nonspecific hydrophobic cinnarizine-Eudragit® interactions seemed to be essential in determining the effect of Eudragit® on cinnarizine supersaturation.

KEY WORDS: supersaturation; cinnarizine; Eudragit S100; precipitation inhibition; permeation.

INTRODUCTION

One of the main reasons for the poor bioavailability of drugs is poor solubility/dissolution in an aqueous medium (1, 2). To overcome this hurdle and enhance the dissolution of drugs in the dissolution medium, a solubilizing agent such as cyclodextrin can be incorporated in the formulations or the drugs can be included inside surfactant micelles (3). However, the solubilization of poorly water-soluble drugs does not always guarantee an enhancement of drug permeation, because the encapsulated drugs are unable to permeate the membranes easily (4).

The second approach is to generate the supersaturated drug solution using salt or amorphous forms of a poorly water-soluble drug (5). As a supersaturated drug solution can create a greater free drug fraction in the medium or gastrointestinal tract, higher free drug fraction in the solution can increase the chance of drug molecules for absorption. Several reports have revealed that the supersaturated approach can be utilized to improve oral absorption of drugs with poor water solubility (6, 7). Some studies show superior improvement in absorption by generating drug supersaturation in the small intestine (8). Weakly basic drugs with poor solubility could easily dissolve in the stomach but as soon as the solution reaches the small intestine, a supersaturated drug solution is formed.

Generally, drugs which are weak bases and with pKa values between 5 and 8 have a high chance to dissolve in the stomach since they exist mainly in the ionized form (high water solubility) due to the acidic state. However, when the

[1] Faculty of Pharmacy and Drug Applied Research Center, Tabriz University of Medical Sciences, Tabriz, 51664, Iran.
[2] Sahand University of Technology, Tabriz, Iran.
[3] Pharmaceutics Research Laboratory, School of Life Sciences, University of Sussex, Brighton, UK.
[4] Student Research Committee, Tabriz University of Medical Sciences, Tabriz, Iran.
[5] Nano Drug Delivery Research Center, Kermanshah University of Medical Sciences, Kermanshah, Iran.
[6] Islamic Azad University, Tehran, Iran.
[7] To whom correspondence should be addressed. (e–mail: mmaghsoodi@ymail.com)

solubilized weak base drug enters the small intestine which is alkaline, partially or completely, the weakly basic drug start precipitating (as the drug would be in an un-ionized form which is less soluble). This implies that the supersaturated solution of weakly basic drugs can be generated in the small intestine (9, 10).

As the supersaturated solution is not stable, the drug can be simply precipitated from such a supersaturated solution resulting in a loss in the supersaturated state advantages.

As the weakly basic compounds might crystallize upon entry into the small intestine, the main challenge is the inhibition of crystallization of weakly basic drugs in the small intestine. It is well demonstrated that if the time to maintain the drug supersaturation is prolonged for an adequate time under physiological conditions, then this can lead to an improvement of drug absorption (11–13). Thus, to preserve the supersaturated drug solution for a longer period, a drug crystallization inhibitor is necessary (14, 15).

Cinnarizine (CIN), as a model compound, was studied in this research. CIN is a weakly basic compound with pKa_1 1.94 and pKa_2 7.47 which dissolves 2 μg/ml at pH 6.5 but dissolves 1000 times more (2110 μg/ml) at pH 1.2. CIN, a lipophilic drug with a partition coefficient of 5.8 (logP), can be categorized as a Biopharmaceutical Classification System Class II drug (16). The poor solubility at higher pH indicates that it is highly likely the proposed drug may partially crystallize upon transfer to the small intestine. A previous research on the bioavailability of CIN has demonstrated that the bioavailability of CIN is very low and unpredictable (17).

The use of polymers in order to inhibit the crystallization of drugs with poor solubility from supersaturated solutions is becoming popular. Furthermore, several studies have shown that polymers are effective to inhibit the crystallization of these drugs from the supersaturated solution for a sufficient time so that the drug absorption can take place before any crystallization occurs (3, 15, 18).

Among polymers, it has been reported that two main polymers namely HPMC and PVP have the main role in the crystallization inhibition of drugs with poor solubility from the supersaturated solutions due to their capability to interact with the drugs *via* hydrogen bonding (19, 20). However, the capability of other polymers to maintain supersaturated solutions and inhibit crystallization is rarely known (21).

Eudragit® polymers are generally utilized in pharmaceutical formulations because of their versatile applications. However, the ability of Eudragit® polymers to inhibit crystallization has not been well studied. Eudragit® polymers can be cationic (Eudragit® E), anionic (Eudragit® L100, Eudragit® L100-55, and Eudragit® S100), and neutral (Eudragit® RL and Eudragit® RS) copolymers. They are based on methacrylic acid and acrylic or methacrylic esters, and they display various degrees of pH-independent or pH-dependent solubility. Eudragit® polymers are being widely used as coating materials for various dosage forms and are extensively used as matrix carriers as well.

With this in mind, in the present research, Eudragit® S100 (Eu), was evaluated for its ability to sustain the supersaturated solution and prevent the crystallization of CIN because it is commonly used as an appropriate enteric polymer in solid dispersion formulations. The understanding of the mechanism by which Eu inhibits CIN crystallization could permit the best design of Eu polymer-based formulations. The CIN permeation study was also conducted using Caco-2 monolayer, which is the generally used membrane to simulate intestinal absorption (22).

MATERIALS AND METHODS

Materials

Cinnarizine (CIN) was obtained from Osvah Pharmaceutical Co, Iran. Eu was obtained from Evonik GmbH, Germany. Hydrochloric acid (HCl), sodium chloride (NaCl), HPLC grade methanol, dibasic potassium phosphate (K_2HPO_4), and monobasic potassium phosphate (KH_2PO_4) were purchased from Merck, Germany. The molecular structures of CIN and Eu are displayed in Figure 1.

Cinnarizine Crystalline Solubility

An additional amount of crystalline CIN was introduced to 100 mM PBS solution (20 ml) with and without pre-dissolved Eu (0.4 mg/ml; our preliminary experiments showed that the inhibitory effect of Eu S100 was improved by increasing its concentration up to 0.4 mg/ml). A thermostatically controlled gas bath shaker was employed to shake the vials at 37°C for 48 h. Each sample was filtered through a 0.45-μm nylon membrane filter, followed by determining the CIN concentration using UV-Vis spectrophotometry set at 253 nm. In addition, altered pH and ionic strength of media were selected as variable factors to assess the effect of Eu on the solubility of crystalline CIN. The solubility of the crystalline form of CIN under different pH levels (6.4, 6.8, and 7.8) and various ionic strengths (0.1, 0.5, and 1 M) at a constant pH of 6.8 was determined. As the solubility of CIN does not change significantly above pH 6, pH levels of 6.4, 6.8, and 7.8 were selected in the current study to make sure an equivalent degree of supersaturation could be achieved from a constant drug concentration at the selected pH levels.

Effect of Eudragit® S100 on the Supersaturation of Cinnarizine

To assess the capability of Eu to maintain the supersaturation of CIN, Eu was pre-dissolved in 100 mM PBS at 0.4 mg/ml in a beaker. CIN was dissolved separately in HCl solution (0.1N) to obtain a 1-mg/ml concentration. To each beaker containing 50 ml of Eu solution, a solution of 1 ml CIN was added to induce an initial CIN concentration of 20 μg/ml. The solution was then vibrated at 100 rpm using a water bath shaker at 37±0.5°C. At different time points (10 min to 120 min), samples were collected and centrifuged at 13,000 rpm (RCF: 16,200 g) for 3 min. This centrifugation condition was used to separate large particles generated during the supersaturation experiment. After centrifugation, large drug particles (crystalline or amorphous) were separated, whereas free CIN and colloidal CIN–rich nanodroplets formed by liquid-liquid phase separation (LLPS) remained in the supernatant. Therefore, the free and colloidal CIN concentration can be determined in the supernatant (23). The obtained supernatant was diluted in a 1:1 ratio with the buffer solution to avoid CIN precipitation and analyzed for

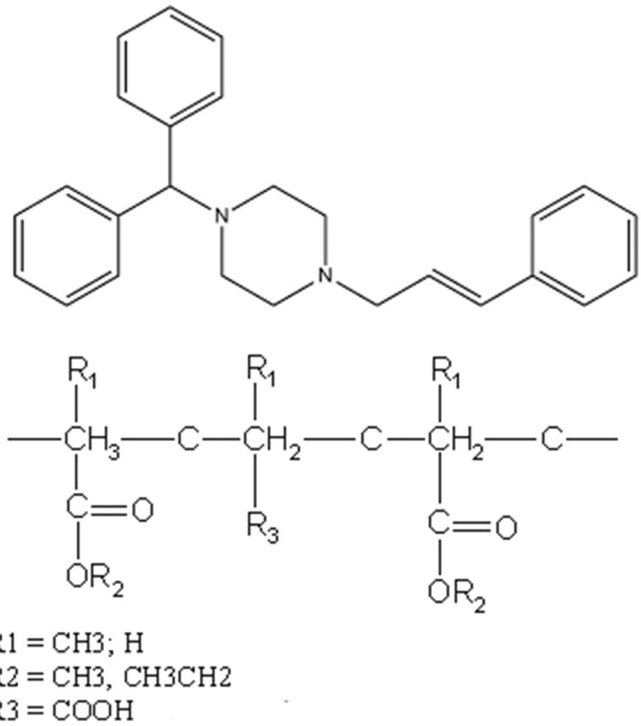

Fig. 1 Molecular structures of CIN (up) and Eu S100 (down)

the concentration of drug by a UV-Vis spectrophotometer (UV-160A, Shimadzu, Kyoto, Japan) at 253 nm. Preliminary results showed that there is no interference between the Eu and CIN assay at 253 nm. In this experiment, the effects of two factors namely pH (6.4, 6.8, and 7.8) and ionic strength (0.1, 0.5, and 1 M) of media were investigated to study the inhibitory effect of Eu on CIN precipitation in a supersaturated solution. The media ionic strength was adjusted with NaCl. The same supersaturation experiments were carried out in the buffer solution without Eu as well.

Aggregation Behavior of Eudragit® S100 Under pH 6.4–7.8

Dynamic light scattering (DLS, Nano ZS, Malvern, UK) was employed to determine the mean particle size of Eu aggregation under pH 6.4–7.8. To prepare samples for DLS, Eu was dissolved in 100 mM PBS under different pH levels to produce a solution of 0.4 mg/ml, then a 0.22-μm nylon membrane filter was used for filtering the solutions. Light scattering was monitored at 90° and determinations were attained at 25°C.

Cinnarizine Amorphous Solubility

Optical density was determined to measure amorphous solubility at 350 nm (24). When the CIN solution stays clear, no extinction occurs; however, when the CIN concentration surpasses amorphous solubility, optical density increases. CIN stock solution was prepared by dissolving the drug (1 mg/ml) in 0.1N HCl solution. The sample solutions were 100 mM PBS with and without 0.4 mg/ml Eu. The various amounts of CIN stock solution were added to sample solutions to produce 5–30 μg/ml CIN concentrations (kept at 37°C), covering the concentration levels lower and higher than the solubility of amorphous CIN. The UV absorbance was measured immediately after making the samples by a UV-Vis spectrophotometer (UV-4802, UNICO, China).

The CIN absorbance at 253 nm was also determined to define whether a rise in extinction at 350 nm was caused by the emergence of drug-rich liquid droplets (where absorbance would be expected to remain high) or crystals (absorbance strongly decreases).

Phase Separation of Cinnarizine Solution

To understand the influence of the degree of supersaturation on supersaturation maintenance and phase separation behavior of CIN solutions, the solutions containing initial drug concentrations of 20, 40, and 80 μg/ml with and without Eu were examined using a supersaturation experiment. The lowest drug concentration examined (20 μg/ml) agrees with the theoretically estimated CIN amorphous "solubility" value (25).

DLS was employed to demonstrate the creation of drug-rich colloids in the supersaturated CIN solution with and without Eu. Aliquots of the solution were assessed instantly after pH shift with DLS.

Transmission electron microscopy (FEI Tecnai Spirit Bio TWIN TEM D1266, USA staining by uranyl acetate) was also employed to view the features of the drug-rich colloids generated by phase separation. For this purpose, the supernatant was collected by centrifugation of the supersaturated CIN solution at 60 min after adding the CIN stock solution.

Powder X-ray Diffraction

The plain CIN and the precipitate of CIN attained from the supersaturation experiment at 2 h were characterized with

powder X-ray diffraction (PXRD). To obtain a sufficient amount of CIN precipitates, CIN solution was made at 5 mg/ml, and 1 ml of this solution was introduced into 50 ml of PBS solution with or without Eu. The solutions were vibrated using a water bath shaker as mentioned previously. After 120 min, the precipitated samples were collected by centrifugation at 13,000 rpm (RCF: 16200 g) for 3 min and vacuum-dried for ~ 1 h. X-ray patterns were obtained using an X-ray diffractometer (Siemens, Model D5000, Germany) equipped with CuKα radiation of wavelength 1.5405 A°, running at 40 kV and 30 mA. Data were obtained over the range of 5.0 to 40.0° 2θ with a scanning rate of 0.06°/min.

Fourier-Transform Infrared Spectroscopy

Fourier-transform infrared (FT-IR) spectroscopy was conducted for the pure CIN, Eu, and CIN-Eu solid dispersion (1:1) using an FT-IR spectrometer (M-B-100, Bomem, Canada) (32 scans for each measurement). Samples were prepared by blending the powder with KBr, followed by compressing it into a disk using a hydraulic FT-IR press. The data was collected between the regions of 1000 and 4000 cm^{-1} at a 4-cm^{-1} resolution.

Differential Scanning Calorimetry

Differential scanning calorimetry (DSC) analysis was carried out on the pure CIN, CIN-Eu solid dispersion (1:1), and physical mixture of CIN-Eu (1:1). DSC-60 (Shimadzu, Tokyo, Japan) was employed to study any changes in the solid-state of materials when being heated. To this end, approximately 5 mg of samples was placed in aluminum crimped pans and the samples were heated from room temperature to 300°C at a heating rate of 10°C/min. The indium was employed to calibrate the instrument.

Preparation of Caco-2 Monolayers

Caco-2 cells were cultured in high glucose Dulbecco's Modified Eagle Medium (DMEM) with 10% FBS. The following materials (1% L-glutamate, 1% nonessential amino acid, 1% penicillin-G, 1% streptomycin, and 0.5% ciprofloxacin) were added to tissue culture flasks under 5% CO_2 and 90% relative humidity at 37°C. Caco-2 cells were washed with fresh medium every other day and passaged weekly (26). The cells were harvested with trypsin-EDTA and seeded onto polyester filters (0.4-mm pores, 4.67-cm^2 growth area) precoated (rat tail collagen) 6-well Transwell cell culture chambers at a density of 180,000 cells/cm^2 (27). Finally, 18–21 days after seeding, when a confluent monolayer was achieved in the culture medium, a Caco-2 cell monolayer was used for permeability tests (28). The transepithelial electric resistance (TEER) of the monolayers was checked routinely before and after the experiment by using a Millicell ERS-2 epithelial volt-ohm meter equipped with STX-2 electrodes to confirm that the integrity of the Caco-2 monolayer has been maintained (28).

Membrane Integrity Measurements

On the day of the permeability experiment, the grown Caco-2 cell monolayers were washed with Hanks balanced salt solution (HBSS) (37°C), then HBSS was added to the apical and basolateral sides. Then, the cells were incubated at 37°C for about 1 h. Following 1 h of incubation, TEER values were measured and used as control values for each sample solution under study. Then, the HBSS in the apical compartment of all inserts was replaced with fasted state simulated intestinal fluid (FaSSIF) containing different CIN or CIN with Eu concentrations, and the cells were incubated again for 3 h. At the end of the incubation period, the TEER of all inserts was measured. TEER percentage was calculated according to the following equations (29).

$$\%\text{TEER} = (\text{TEER at time 3h})/(\text{TEER at time 0}) \times 100$$

Permeation Through Caco-2 Monolayer

To assess the permeation rate of CIN, the culture medium was first removed, and then cells were washed with HBSS. The permeation studies in the apical and basolateral compartments of the Caco-2 monolayer were added to HBSS 30 min before conducting and pre-incubation of the cells in the humidified atmosphere of 5% CO_2 at 37°C. During the transport experiments, the buffer in the basolateral compartment was replaced with 2.6 ml of fresh HBSS buffer, which was adjusted by 10 mM HEPES at pH 7.4 and contained 25 mM glucose. To provide sink conditions, TPGS with a concentration of 0.2% was added to the medium, and in the AP FaSSIF was used as the supersaturated medium; this material was prepared from the original simulated intestinal fluid (SIF) powder using KH_2PO_4 buffer and its pH was adjusted by NaOH 1 M to 6.5. To investigate the effect of the presence of Eu on cell permeability, an appropriate amount of Eu was dissolved in FaSSIF medium to obtain a concentration of 0.4 mg/ml of Eu in the medium, then 1.4 ml of the prepared media was added to the apical section. The solvent shift method was used to create the supersaturation of the drug. Different degrees of supersaturation (DS) (10, 20, and 40) were induced based on the equilibrium solubility of CIN in FaSSIF. For example, the concentration of the solution at DS10 is 10 times the equilibrium solubility of CIN. Throughout the experimentation, the cells cope was kept in an incubator with an orbital shaker at 60 RPM and 37°C and only taken out for sampling. A certain amount of the solution in the BL (0.1ml) was withdrawn at different time points (30, 60, 90, 120, and 180 min) and centrifuged immediately to remove precipitated CIN. The obtained supernatant was analyzed by isocratic high-performance liquid chromatography (HPLC) with UV-Vis detection (HPLC/UV-VIS). All experiments were repeated three times (29). The permeation rate (normalized flux) J was calculated with the formula $J = 1/A \times dc/dt$, where A represents the surface area of the filter and dc/dt is the flux (26).

Quantification of Cinnarizine by HPLC/UV-VIS

An isocratic HPLC equipped with a quaternary pump and UV-Vis detector (Ultimate 3000; Dionex Company) was employed to determine CIN concentrations. The HPLC column was C18 Eclipse (5 μm, 4.6 mm×100mm). A mixture of methanol and KH_2PO_4 buffer (0.05 M and pH 4.5) with a ratio of 65:35 *v/v*% was used as a mobile phase. The volume of injection was set at 10 μl, and the flow rate of the mobile phase through the column was 1 ml/min. The peak area of the drug was measured at a wavelength of 253 nm (29).

Statistical Evaluation of Data

The data were reported as the mean ± standard deviation (SD) of at least 3 determinations. The analysis of variance (ANOVA) followed by the Mann-Whitney *U* test was used to show the difference between the data obtained. The difference was considered statistically significant where p is < 0.05.

RESULTS AND DISCUSSION

Cinnarizine Solubility (Crystalline Form)

Before assessing the supersaturation and crystallization behaviors of CIN, the solubility of the crystalline form of CIN under different pH levels (6.4–7.8) was determined. The solubility of crystalline CIN was measured in a buffer solution in the presence or absence of Eu. It was found that the solubility of the crystalline form of CIN in buffer solution without Eu stayed constant at ~2 μg/ml under pH 6.4–7.8, where CIN was predominantly unionized. This was consistent with the findings of the previous studies (16, 30). The equilibrium solubility of CIN in the presence of 0.4 mg/ml Eu was also determined. This Eu concentration corresponds to the polymer concentration tested in the supersaturation experiments in the current study. In Eu polymer solution, no significant change in CIN solubility was observed, and no substantial difference in concentration of CIN at different pH levels was found. The solubility of crystalline CIN was also determined under various ionic strengths (0.1–1 M) at a constant pH of 6.8 (simulated pH for small intestine), and the results showed no significant difference in the solubility of the crystalline form of CIN at any of the ionic strengths tested.

Supersaturation Experiment

According to previous studies, the effectiveness (E) of polymers in inhibiting the crystallization of drugs is dependent on the initial degree of supersaturation (31, 32). Therefore, since supersaturation has an essential role as a driving force for crystallization, an equivalent degree of supersaturation is important when evaluating the E of the polymer at different conditions in maintaining the supersaturation of drugs. E value of Eu on maintaining supersaturation of CIN under different pH levels (6.4, 6.8, and 7.8) and ionic strengths (0.1, 0.5, and 1 M) was investigated at CIN concentration of 20 μg/ml. As it was shown that the solubility of CIN remains unchanged, an equivalent degree of supersaturation could be achieved from a constant drug concentration.

E value of Eu in inhibiting precipitation of CIN was assessed using the following equation:

$$E = \frac{(AUC)p}{(AUC)a}$$

where $(AUC)_p$ and $(AUC)_a$ are the integrated areas under supersaturation curves up to 2 h in the presence and absence of Eu, respectively. Eu with $E \leq 1$ was supposed to be an ineffective precipitation inhibitor, while Eu with $E > 1$ was considered a precipitation inhibitor.

The impact of the ionization state of the Eu on its effectiveness in inhibiting the crystallization of the CIN was examined by comparing supersaturation maintenance for the drug at three pH levels (6.4, 6.8, and 7.8), and the results are presented in Figure 2. As expected, in the absence of the polymer the supersaturation maintenance of CIN is comparable at pH 6.4, 6.8, and 7.8 (Figure 2a). CIN quickly precipitates in a buffer solution without the presence of Eu irrespective of the solution pH, while Eu sustained CIN supersaturation, depending on solution pH. The results showed that the capability of Eu to increase the supersaturation of CIN was determined by the pH of the solution, and the concentration of CIN in Eu solution was far above the solubility of crystalline CIN (~2 μg/ml) at various pH levels. As seen in Figure 2, a noticeable improvement in CIN supersaturated concentration (12 ~ μg/ml) after 2 h was observed at pH 6.4 compared to pH 7.8.

Figure 2b compares $(AUC)_p$ to $(AUC)_a$ for CIN at an initial concentration of 20 μg/ml at different pH levels. This figure shows that Eu had similar E values when the pH was 6.4 or 6.8 (in both cases, E was 4). When pH was increased to 7.8, the E value decreased to 2.

The E value of Eu as a precipitation inhibitor cannot be related to a change in supersaturation as the solubility of crystalline CIN was observed to be ~2 μg/ml, independent of the presence of Eu and the pH of the solution.

It has been proven that maintaining the supersaturated concentration of a drug by polymers is mainly because of the drug-polymer molecular interaction (33, 34). When an attractive drug-polymer interaction occurs, the nucleation and subsequently crystal growth rate of the drug can be slowed down. This in turn impedes precipitation and maintains the supersaturated concentration of the drug (35). Many earlier investigations have indicated that the inhibitory effect of polymers on drug crystallization is strongly correlated with polymer hydrophobicity. In the case of a very high hydrophilic polymer, it is probable to interact more favorably with water, resulting in a poor crystallization inhibition efficiency. In brief, the degree of hydrophobicity of polymer mostly determines the magnitude of adsorption of polymer to the newly generated drug nuclei surface, which accordingly influences the inhibitory effect of the polymer on drug crystallization (36, 37).

The inhibitory effect of Eu on CIN crystallization at different pH levels can be explained in terms of the hydrophobicity of the polymer. Eu as a pH-sensitive polymer is a macromolecule containing potential ionizable groups.

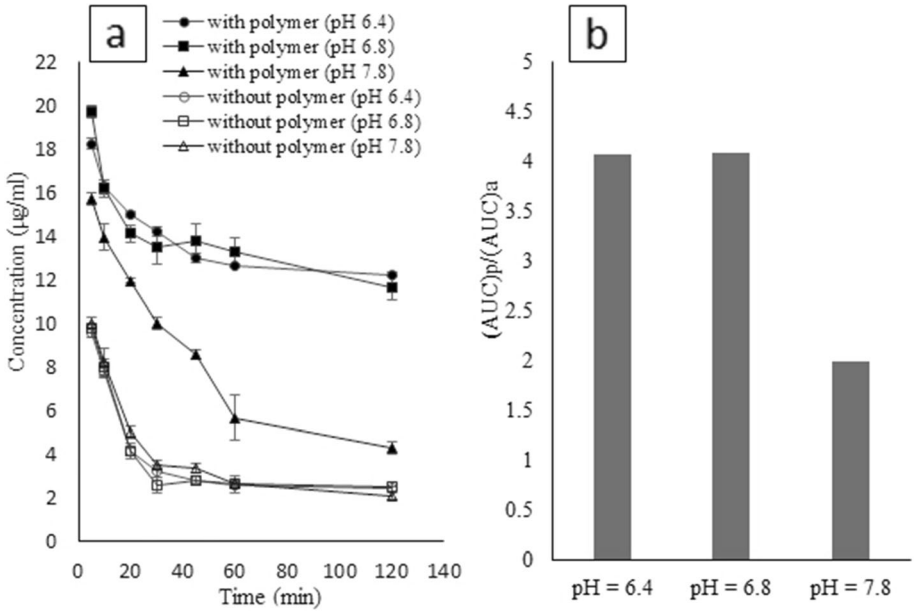

Fig. 2 Drug concentration profiles of CIN under different pH (6.4–7.8) levels during supersaturation experiments with and without the presence of Eu (**a**). Effectiveness of Eu under different pH levels (**b**)

Therefore, at different pH values, the polymer ionization degree and consequently its solubility would change (38).

Eu is a copolymer of methyl methacrylate (MMA) as an ester group with methacrylic acid (MA) with the molar ratio of two monomers 1:2 (MA:MMA) (39). Carboxylic groups of methacrylic acid moiety can strongly influence the hydrophobicity of the anionic Eu polymer due to the ionization and transformation to carboxylate ions. Therefore, the low effectiveness of Eu on maintaining the supersaturation of CIN at pH 7.8 could be because of the high ionization of polymer at this pH which is higher than polymer's minimal dissolving pH (pH 7). In other words, the hydrophobicity of Eu increases as the pH of the medium decreases as a consequence of protonation of carboxylate function to carboxylic and thus less ionized hydrophilic groups. As mentioned above, it is well known that higher polymer hydrophobicity increases polymer-hydrophobic drug affinity, exhibiting stronger crystallization inhibition and subsequently greater supersaturation. Therefore, Eu is assumed to be more hydrophobic at lower pH, hence improving the binding affinity and interaction with hydrophobic drugs, resulting in more efficient crystallization inhibition. In the other words, increasing the hydrophilicity of Eu (derived from the ionization of carboxylic groups) decreased its affinity of hydrophobic interaction with the drug at pH higher than the pH where Eu start dissolving (pH >7). In conclusion, the inhibition effect of Eu on CIN crystallization was influenced by the carboxylic acid substitutes that could be ionized in an aqueous solution. Several studies have also drawn similar conclusions regarding the effect of polymer ionization on inhibiting drug precipitation (40, 41).

In this work, the importance of hydrophobic interaction between Eu and CIN was further investigated by changing the ionic strength of media (0.1, 0.5, and 1 M) at a constant pH of 6.8. It has been shown that when the ionic strength of a solution is increased by the addition of salts, it is anticipated that the polymer molecules with hydrophobic groups are adsorbed more strongly onto the surface of the hydrophobic drug (42).

As shown in Figure 3a, in the absence of Eu, CIN quickly precipitates from supersaturated solution irrespective of the solution ionic strength; however, Eu maintained CIN supersaturation, depending on solution ionic strength.

Figure 3b shows that ionic strength has a significant effect on the performance of Eu in inhibiting precipitation where a higher ionic strength increased the performance of Eu (1 > 0.5 > 0.1 M). In other words, the higher ionic strength of the medium enhanced the influence of Eu on supersaturation maintenance of CIN, suggesting that the hydrophobic forces have a dominant role in CIN-Eu interaction. Some earlier studies have reported similar results and demonstrated that hydrophobic forces that drive interaction with the hydrophobic drug are improved by increasing ionic strength where the efficiency of the polymer was increased (32, 38, 39). For example, Shi *et al.* have found that felodipine crystallization inhibition by cellulosic polymers was greatly influenced by changes in the ionic strength of the medium (43).

Aggregation Status of Eudragit® S100 Subjected to Various pH Levels (6.4–7.8)

Earlier studies have revealed that the polymer aggregation properties might relate to their supersaturation preserving capability (44). Therefore, it is assumable that aggregation properties of Eu in an aqueous solution could impact its potential for interaction with CIN molecules, hence influencing its ability to inhibit the crystallization of CIN. Eu as an enteric polymer is an amphiphilic molecule containing hydrophobic and hydrophilic regions. The hydrophobic region may potentially interact with hydrophobic molecules, generating nano-sized agglomerates, whereas the hydrophilic

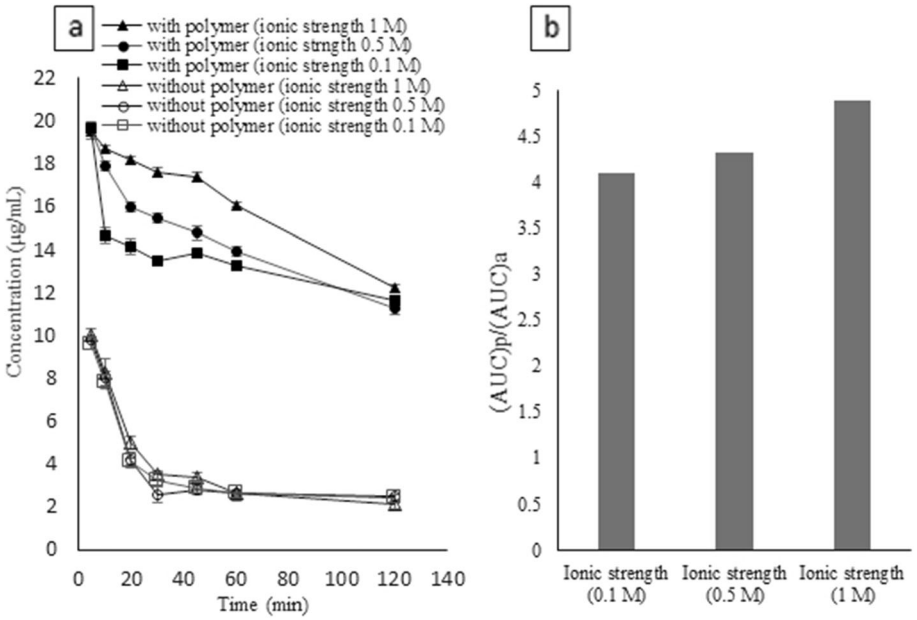

Fig. 3 Drug concentration profiles of CIN under different ionic strengths (0.1–1 M) during supersaturation experiments with and without the presence of Eu (**a**). Effectiveness of Eu under different ionic strengths (**b**)

region may create repulsion to reduce the generation of big agglomerates (45). Carboxylic groups on Eu could increase the hydrophilicity of the anionic Eu polymers due to the ionization and transformation to carboxylate ions, while ester functional groups contribute to the hydrophobicity of the Eu (39). Ester functional groups as hydrophobic regions potentially work in hydrophobic interaction with drug molecules, while carboxylic groups as hydrophilic regions enable the creation of hydrated nanoparticles in an aqueous solution. Therefore, understanding Eu aggregation properties could be useful to reveal its mechanisms of preserving CIN supersaturation. To this end, dynamic light scattering (DLS) was employed to measure the hydrodynamic particle size of Eu in solutions under various pH levels (6.4–7.8), and the results are shown in Figure 4. According to the results, the particle size of Eu was not affected by increasing pH from 6.4 to 6.8. The particle size noticeably dropped when the pH of the Eu solution was increased to 7.8.

When pH was increased to 7.8, Eu particle size distribution showed bimodal distribution. The extra particle size peak at lower size could be due to the appearance of small aggregates of Eu in the solution. The appearance of small aggregates at high pH (7.8) could be due to better solubility of Eu at above pH 7, as the dissolution of more Eu particles could alter the polymer hydration or ionization of Eu polymer in the solution.

One study similarly found that HPMC-AS polymers have lower aggregation numbers just as the pH has been raised by 0.5 units higher than the pH needed to dissolve the polymer (46). They have pointed out that at a pH higher than the pH that polymer dissolves easily, the polymer particles can be entirely hydrated or ionized, which led to smaller particle sizes. Additionally, a similar phenomenon was found for organic molecules with ionizable functional groups where unionized and ionized forms have changed significantly at pH close the pKa of the organic molecules and after that stayed approximately constant as the pH further changed (47).

A reduction in the particle size of aggregates of Eu when pH increases could be a consequence of decreased hydrophobicity or increased polymer hydration under higher pH as higher carboxylic components of Eu were ionized. These changes of the Eu could subsequently increase its interaction with solvent molecules. As expected, Eu showed significantly lower effectiveness (E=2) at pH 7.8 when Eu aggregated into smaller sizes, representing that the Eu polymer becomes less hydrophobic therefore decreasing CIN-Eu polymer hydrophobic interactions, and consequently lowering drug supersaturation. Compared to pH 7.8, under pH 6.4 and 6.8, Eu aggregated similarly into larger sizes which may designate a higher hydrophobicity or polymer-polymer interaction, which causes higher binding affinity and hydrophobic interaction with the drug molecules in solution and consequently higher effectiveness (E=4). These results further confirm the importance of polymer-drug hydrophobic interactions for Eu.

Solubility of Amorphous Cinnarizine

Before assessing the phase separation performance of supersaturated CIN solutions, the solubility of the amorphous CIN was determined. The main reason for this solubility measurement is that it determines the threshold concentration of CIN where phase separation might occur. The amorphous CIN solubility was measured with and without the presence of Eu at pH 6.8 by the UV absorbance/extinction method (4) and determining the absorbance and optical density of the solution at 253 and 350 nm, respectively (Figure 5).

The solubility result of CIN in the presence of Eu was shown in Figure 5a. It could be considered that the relationship between CIN concentration and absorbance at

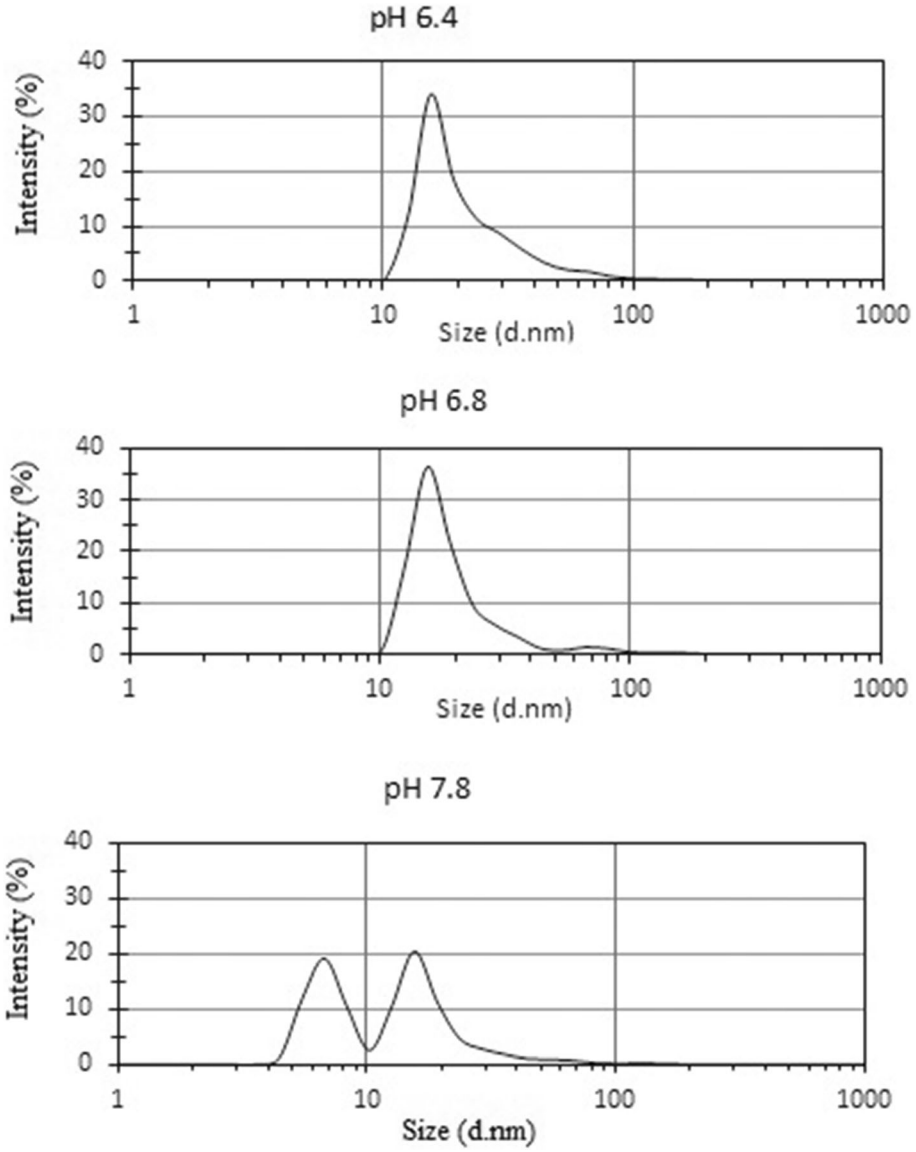

Fig. 4 Particle size distribution for Eu under pH 6.4–7.8 measured by DLS

253 nm was linear, but the linearity was lost at 22 μg/ml. The optical density at 350 nm was insignificant up to 22 μg/ml; however, beyond this concentration, it displayed a linear rise, demonstrating the creation of a scattering phase. Therefore,

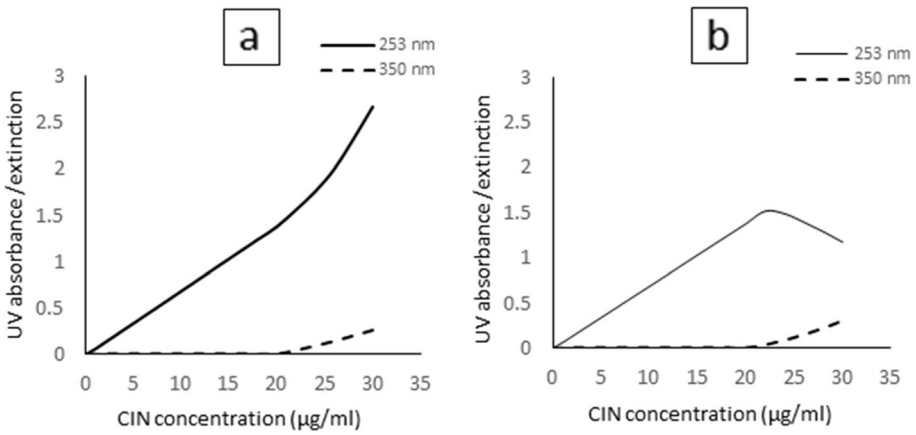

Fig. 5 UV absorbance at 253 nm and extinction at 350 nm as a function of CIN concentration in the presence of 400 μg/ml, Eu (**a**) in the absence of polymer (**b**)

for buffer solution in the presence of Eu, the amorphous solubility of CIN was about 22 μg/ml, consistent with the estimated theoretical solubility of amorphous CIN (25). The solubility of the amorphous form of a drug signifies the LLPS threshold concentration above which drug-rich nanodroplets are generated. In the presence of Eu, LLPS might happen when CIN concentration surpassed 22 μg/ml. The happening of LLPS at CIN concentration of greater than 22 μg/ml (at pH 6.8) was also supported by DLS results. In the presence of Eu, which was added to inhibit CIN crystallization, a scattering phase of 100–250 nm diameter was detected at CIN concentrations of 40 and 80 μg/ml.

The LLPS threshold concentration could not be defined without the presence of Eu due to the fast precipitation of CIN from the supersaturated solution, which led to a fall in absorbance and a simultaneous nonlinear rise in extinction (Figure 5b). A great extinction measured at 350 nm was attributed to the generation of many small CIN crystals which were distinguishable by visual control.

Phase Separation of Cinnarizine Solution

To study the influence of the degree of supersaturation on the supersaturation maintenance and the phase separation behavior of CIN solution, the supersaturated solutions containing initial drug concentration of 20, 40, and 80 μg/ml (representing the DS of 10, 20, and 40, respectively) with and without the presence of Eu were evaluated.

According to the theoretical concerns, the nucleation rate of the compound in the supersaturated state greatly depends on the initial level of supersaturation. The supersaturated solution is inherently thermodynamically unstable and hence the drug precipitation takes place over time (48, 49). In other words, the supersaturated solutions with a higher level of supersaturation tend to nucleate and precipitate faster from the solutions, as the greater degree of supersaturation of a drug acts as a driving force for precipitation.

The effect of the initial degree of supersaturation on supersaturation maintenance of CIN with and without the presence of Eu is revealed in Figure 6a. Without the presence of Eu, as expected, the results verified that the maintenance of CIN supersaturation was influenced by the initial drug supersaturation level and the increased initial degree of supersaturation led to an increase in the maximum attainable CIN concentration ($p<0.05$). However, a faster rate of CIN precipitation (reflected by steeper slopes) was observed as the initial concentration increased. Therefore, the higher initial level of supersaturation will not consistently lead to better performance. Findings from this study are consistent with the results published elsewhere (50, 51). Figure 6a shows that Eu effectively sustained supersaturation of CIN at all of the supersaturation levels tested.

Earlier studies have demonstrated that the inhibition effect of polymers on drug precipitation is influenced by the initial degree of drug supersaturation, and polymers show only slight inhibitory action at the very high levels of supersaturation (31, 32, 40). According to obtained results, a similar trend occurs for Eu and CIN studied in the current research and the effectiveness of Eu was reversely influenced by the level of supersaturation. The highest effectiveness factor ($E=4$) for Eu was found at DS of 10, the lowest level of supersaturation tested for CIN, compared to effectiveness factors of about 2.6 and 2.0 at DS of 20 and 40, respectively (Figure 6b).

The phase separation behavior of CIN solution as a function of the degree of the supersaturation was investigated using DLS analysis to characterize the nanoparticles generated upon LLPS. It has been shown that a higher level of supersaturated solution of a drug might undergo LLPS when its crystallization is efficiently prevented (24). The threshold LLPS concentration has been demonstrated to be in good agreement with the amorphous solubility (52, 53). When supersaturated solutions of drugs undergo LLPS, they generate a colloidal drug–rich nanodroplet phase, and this colloidal phase coexists with an aqueous phase with a concentration equivalent to the amorphous solubility of the drug. The nanodroplets generated in the amorphous solubility are typically in the size range from 100 to 500 nm when characterized instantly after creation (54–56). The lowest concentration of CIN, which generates the initial CIN concentration of 20 μg/ml (DS of 10), was the first system assessed. The obtained CIN concentration without the presence of Eu rapidly declined after pH shift. However, in the presence of Eu, the CIN concentration gradually reduced. DLS analysis of the solution at DS of 10 in the absence and presence of Eu instantly after pH shift demonstrated the lack of nanoparticles. This is predictable because the initial CIN concentration of this solution was less than its amorphous solubility and consequently LLPS was unlikely to occur. In the case of DS of 20 and 40, after pH shift, and without the presence of Eu, CIN precipitated rapidly.

For all the supersaturation ratios, nanodroplets could not be detected in the absence of Eu due to the quick precipitation that happened during the addition of the stock CIN solution which resulted in a clear solution with observable crystals. The formation of crystals was also demonstrated by the amorphous solubility determination in absence of Eu, wherein a concurrent nonlinear rise in extinction and fall in absorbance was observed. In the presence of Eu at DS of 20 and 40, the solution appears to be milky which is easily visible to the naked eye (Figure 7).

As the amorphous solubility of CIN was measured to be 22 μg/ml, at DS of 20 and 40, the initial CIN concentrations in solutions (40 and 80 μg/ml, respectively) surpassed the solubility of amorphous form; therefore, LLPS may occur and produce colloidal drug-rich phase in the presence of Eu added to inhibit CIN precipitation. DLS analysis of the obtained supernatant after pH shift demonstrated that the nanoparticles as scattering phase appeared in the size range from about 100 to 250 nm at DS of 20 and 40 in the presence of Eu.

TEM was employed to support the generation of nanoparticles in the supersaturated solution of CIN at DS of 20 and 40 in the presence of Eu. As shown in Figure 8, in these cases, spherical nanodroplets were easily observable by TEM. In contrast, no particles can be seen in solution in the absence of Eu, where CIN precipitation was fast (data not shown).

The obtained results demonstrated that (a) for the supersaturated solution of CIN above, its amorphous solubility with the presence of Eu, CIN-rich nanodroplets appeared; (b) nanodroplets did not form with CIN supersaturation less

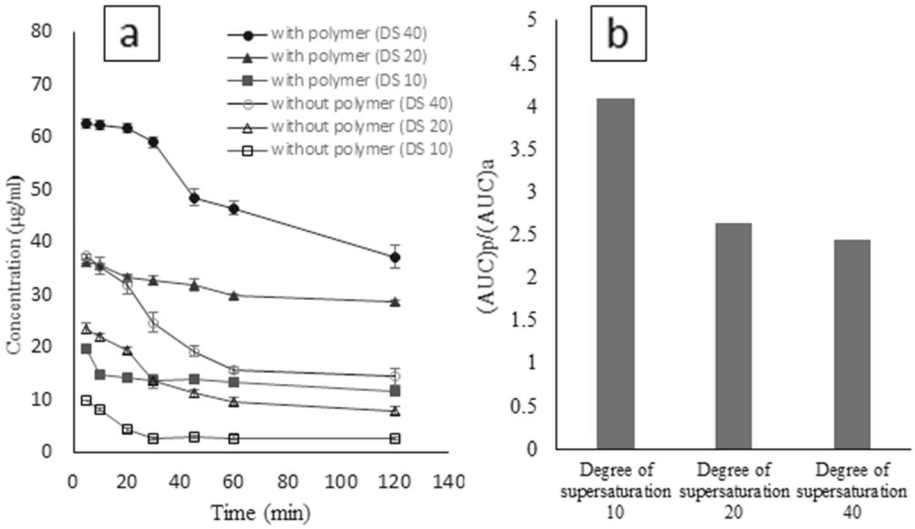

Fig. 6 Drug concentration profiles of CIN at different degrees of supersaturation with and without the presence of Eu (**a**). Effectiveness of Eu at different degrees of supersaturation (**b**)

than its amorphous solubility and c) for the supersaturated solution above amorphous solubility in absence of Eu, no nanodroplets appeared. Therefore, it can be concluded that LLPS happens when supersaturated solution surpasses the amorphous solubility of the drug and whereby precipitation is inhibited. LLPS may never occur in a supersaturated solution that undergoes fast precipitation. These findings are in agreement with the results of earlier studies (57, 58). A supersaturated solution which undergoes LLPS could exhibit superiority in terms of *in vivo* absorption. It is worth noting that by increasing drug supersaturation greater than the solubility of its amorphous form, when LLPS happens, the maximum achievable free drug concentration could be maintained in solution as long as the drug-rich nanodroplets exist, because the drug-rich droplets could quickly replenish absorbed free drug in the small intestine, thus effectively sustaining the absorption of drug (54, 55).

PXRD of the Precipitates of Cinnarizine

To elucidate the supersaturated state of CIN in the presence of Eu, the solid state of the precipitated CIN was evaluated by PXRD analysis. Plain CIN had a crystalline structure as demonstrated by the presence of well-defined peaks at 2θ of 10.32, 13.34, 14.70, 18.22, 20.91, 22.02, and 24.82 (Figure 9). PXRD patterns of plain CIN powder were in agreement with the published research article (59). The precipitate of CIN was observable after being prepared at all degrees of supersaturation. PXRD of the precipitated CIN showed that some of the representative peaks of CIN are evident, verifying that the crystalline structure of the precipitated CIN was not entirely lost (Figure 9). The peak position and overall appearance of the PXRD patterns of the precipitates obtained under different pH levels were quite similar.

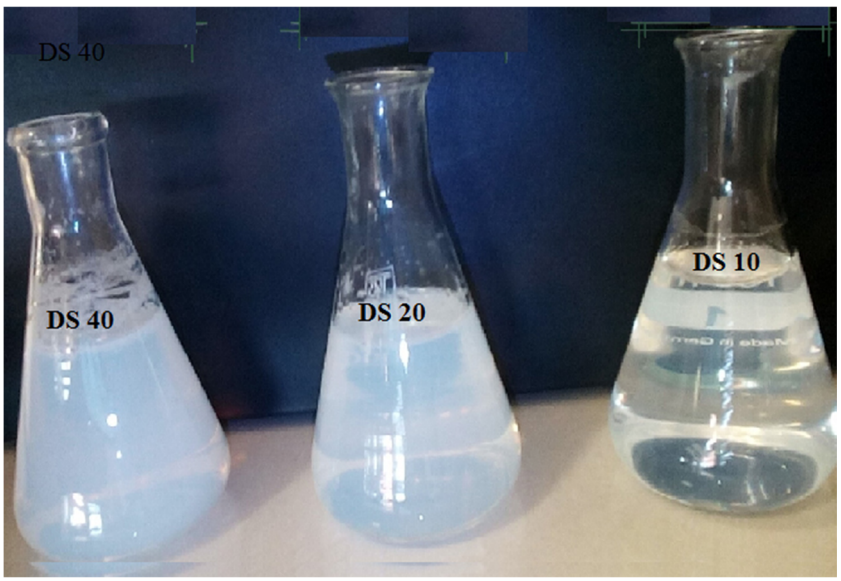

Fig. 7 The appearance of CIN solution at different degrees of supersaturation in the presence of Eu

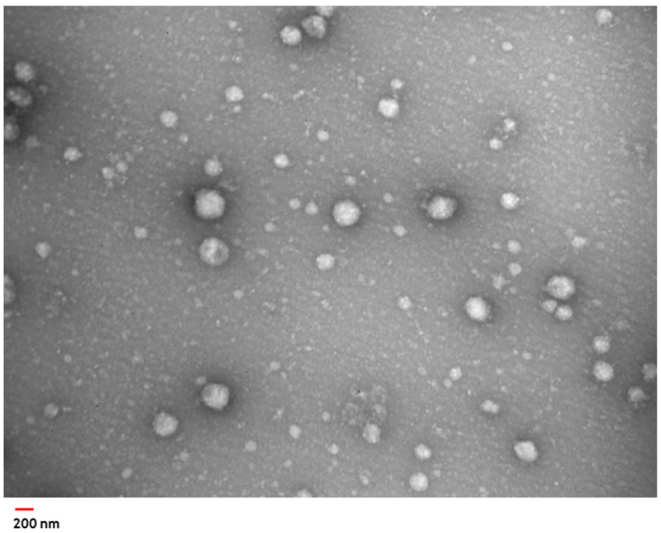

Fig. 8 TEM image for supersaturated CIN solution at DS 20 in the presence of Eu

FT-IR and DSC Analysis

It has been shown that the polymer adsorption onto the surface of drug crystal, a necessary step for inhibition of crystal growth, is mainly caused by hydrophobic interactions (36, 37). In the present study, the importance of drug-polymer hydrophobic interactions for Eu was tested by varying pH and ionic strength and the obtained results suggest that CIN-Eu hydrophobic interactions play an important role in determining Eu effectiveness on the precipitation inhibition of CIN from its supersaturated solutions.

Furthermore, polymer-drug interactions such as hydrogen bonding may also have a significant role in controlling drug crystal growth if drug and polymer bear acceptor and donor groups (60, 61). FT-IR analysis can be employed to provide evidence for specific drug and polymer interactions. Eu displayed specific bands of the C=O in the case of the esterified carboxylic group and the carboxylic acid group at 1730 and 1700 cm^{-1}, respectively (62). According to C=O group of Eu in Figure 10, a shift was detected in the position of the C=O stretching vibration bands in CIN: Eu (1:1) solid dispersion sample. The pure CIN showed a characteristic band of the C-N stretch at 1136 cm^{-1} (59). As seen in Figure 10, the position of the C-N peak of CIN (at 1136 cm^{-1}) in CIN-Eu (1:1) solid dispersion formulation was also shifted, signifying the difference in CIN hydrogen bonding environment. These changes could be evidence for a possible hydrogen bonding between the C-N group of CIN and the C=O group of Eu. The results of the FT-IR demonstrated that Eu polymer may also interact with CIN by specific interactions.

The DSC thermograms of the pure CIN, CIN-Eu solid dispersion (1:1), and physical mixture of CIN-Eu (1:1) are shown in Figure 11. The DSC traces for all samples displayed

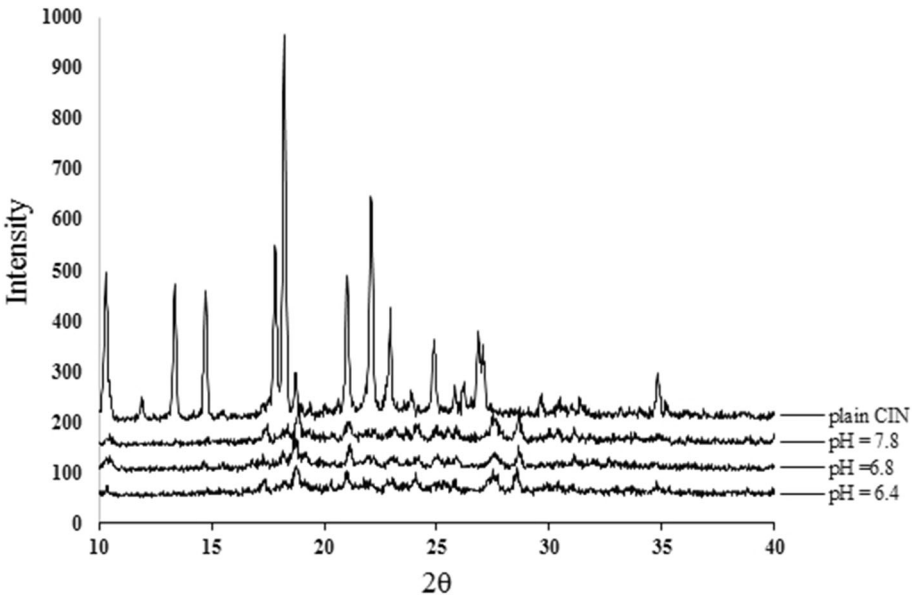

Fig. 9 XRPD of CIN from plain powder and precipitate obtained from supersaturation experiments in the presence of Eu under different pH levels

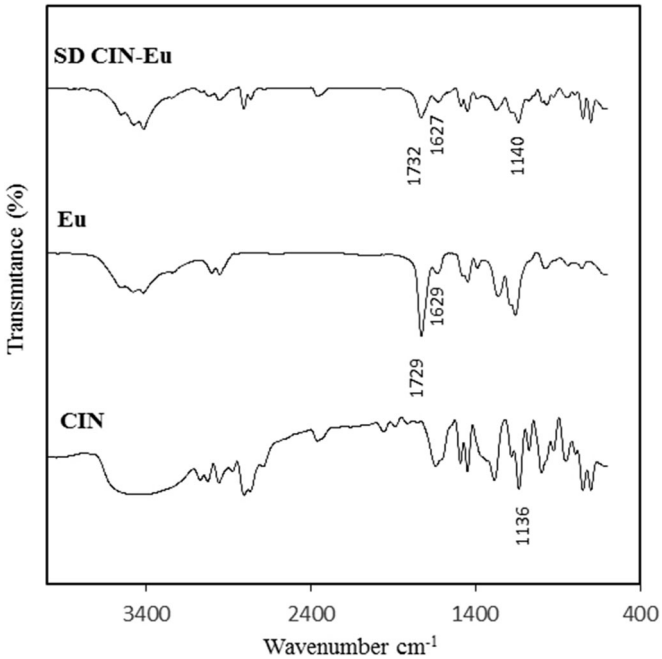

Fig. 10 FT-IR of the spectrum of CIN, Eu, and binary solid dispersion (SD) of CIN-Eu (1:1)

a single endothermic peak at 119°C, consistent with the melting point of CIN. However, in the case of CIN-Eu solid dispersion (1:1), a smaller melting peak of CIN was observed compared to a physical mixture of CIN with Eu (1:1). This change could be a result of partial dispersion of CIN within Eu because of the interaction between drug and polymer. In conclusion, these interactive forces-nonspecific hydrophobic CIN-Eu interactions and specific interaction (hydrogen bonding) at the molecular level are likely to be responsible for the inhibitory effect of Eu which inhibits any physical modification of CIN molecules such as crystallization and consequently stabilize CIN molecules in solution (63).

Permeation Through Caco-2 Monolayer

The positive effect of Eu on supersaturation maintenance of CIN solution was demonstrated in the supersaturation experiments. The supersaturation experiments demonstrated that the presence of Eu (0.4 mg/ml) sustained the supersaturated state of the drug for 2 h, but without the presence of polymer, the drug quickly precipitated. However, it should be kept in mind that the *in vitro* estimation of supersaturation and precipitation can be estimated precisely if it is associated with absorption devices, as in several cases, the supersaturation value can be underestimated by the supersaturation experiments. The reason for more extensive supersaturation of a drug in the existence of absorption devices may be that permeation can act as a substitute for precipitation. For this reason, in what way supersaturation impacts the transport of CIN *in vitro* across Caco2 cells in the presence of Eu was assessed. The permeation of CIN through the Caco-2 membrane at various concentrations of CIN was displayed as a flux rather than as the apparent permeability because valid the apparent permeability determinations need that the drug concentrations in the donor side are identified; however, measurements of the drug flux through the membranes is not dependent on the drug concentration in the donor side. In the case of poorly water-soluble drugs, the precise initial concentration of the dissolved drug was not identified due to their quick precipitation when supersaturation was generated. Earlier studies have reported the same finding for some other drugs (64–66).

The influence of inducing various levels of supersaturation on the transport of CIN across the Caco-2 cell membrane is exhibited in Figure 12. The cumulative amount of CIN in the acceptor basal side is displayed as a function of time. As shown in Figure 12a, there is a lag time in the permeation of the drug to the basal side which could be attributed to the time required to saturate the Caco-2 membrane prior to attaining steady flux, as demonstrated by earlier studies (64).

The addition of 0.4 mg/ml Eu to the apical side led to the higher amount of CIN moving toward the basal side. Moreover, the flux of CIN was considerably increased in the presence of polymer in comparison to no polymer ($p < 0.05$) (Figure 12b).

Considering the results of supersaturation experiments, it can be assumed that the amount of CIN dissolved on the donor compartment was higher with the presence of Eu compared to when there is no polymer involved.

In the presence of Eu, the maximum amount of CIN transported to the basal side was over 2 h, and the maximum resulting flux was highest when DS was 40. This was consistent with the supersaturation experiment in which the highest level of supersaturation (DS 40) provided the maximum concentration of CIN after 2 h.

It has been shown that higher drug concentration on the apical donor compartment as a consequence of solubilizing the additives may not result in a corresponding increase in the flux in all conditions and the outcome can be influenced by the properties of the drug and drug-additive interaction. In many studies, it has been reported

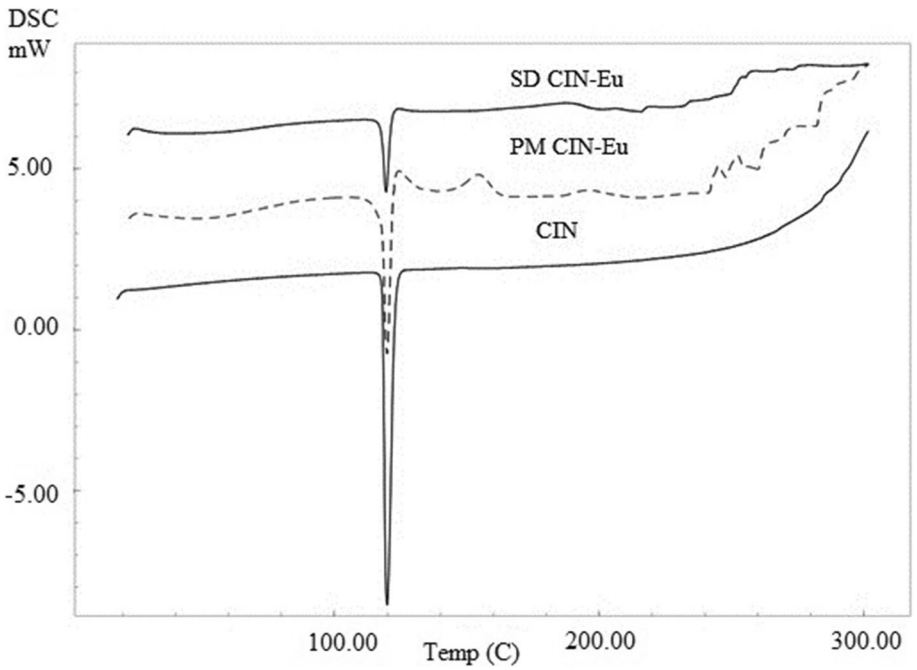

Fig. 11 DSC scans of the samples: plain CIN, binary solid dispersion (SD) of CIN-Eu (1:1 ratio), and physical mixture (PM) of CIN and Eu (1:1 ratio)

that the presence of some additives in the donor apical compartment exerts an undesirable impact on permeation, which is explained by the fact that micellar solubilization by additives increases the apparent solubility of the drug resulting in an overestimation of the exact supersaturation value, hence not resulting in raising the permeation rate (67, 68). However, opposite to these findings, the current permeation studies demonstrated that Eu (0.4 mg/ml) on the apical side markedly increased the cumulated CIN concentration permeated through Caco-2 cells after 2 h, and attained the higher flux.

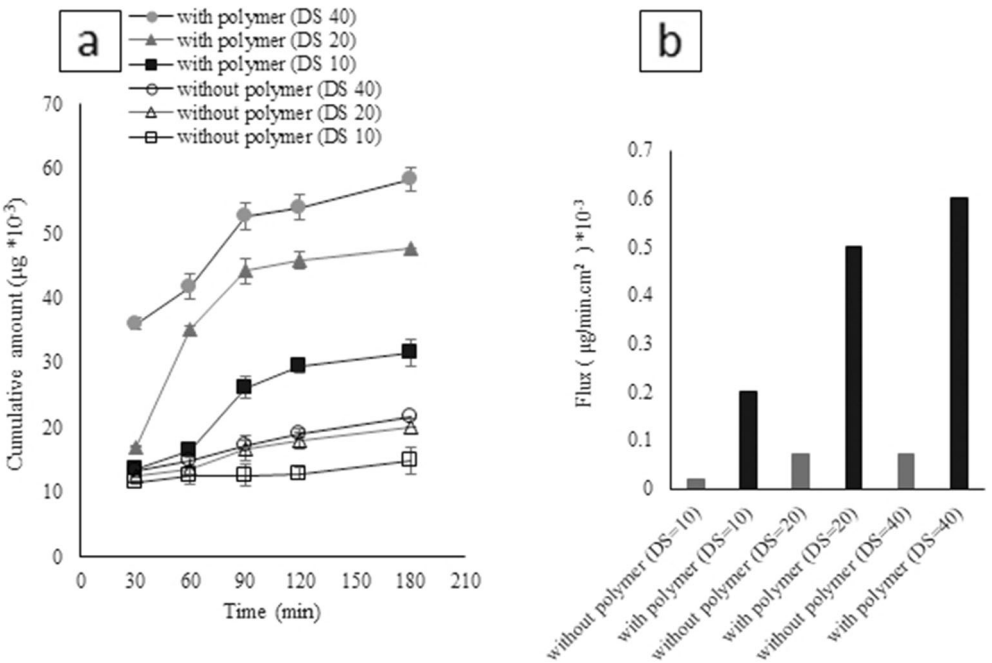

Fig. 12 Cumulative amount of CIN recovered from the basolateral acceptor after transport across Caco-2 cell monolayer upon induction of different degrees of supersaturation in the apical compartment with and without the presence of Eu (**a**). Calculated flux across Caco-2 cell monolayer in the absence and in the presence of Eu at different degrees of supersaturation (**b**). Data represent means ± SD (n=3)

CONCLUSION

In this study, the stabilization mechanism of CIN supersaturation by Eu was revealed. The effectiveness of Eudragit® was demonstrated to be dependent on the pH and ionic strength of the solution. The results proved that higher drug supersaturation was maintained by Eudragit® when lower pH or higher ionic strength was used. Decreasing pH (from 7.8 to 6.4|) and increasing ionic strength (from 0.1 to 1 M) result in less ionized carboxylic groups; thus, Eudragit® becomes more hydrophobic. This in turn can increase its affinity with CIN as a hydrophobic drug, which causes higher cinnarizine supersaturation with stronger precipitation inhibition. The current study demonstrated that Eudragit® formed aggregates in solutions and a relationship was found between the particle size of Eudragit® aggregates and its impact on the supersaturating of cinnarizine. The obtained results suggest that cinnarizine-Eudragit® hydrophobic interaction is a determining factor for Eudragit® effectiveness. Permeation studies using Caco-2 cells revealed that improvement of cinnarizine supersaturation by Eudragit® allowed a marked enhancement in the transport/flux. This study can permit researchers to comprehend the behavior of Eudragit®-based formulations in the gastrointestinal tract and to develop the optimal formulation proportional to Eudragit® character. While the current results are valid for cinnarizine and anionic Eudragit®, the authors suppose that such a mechanism would also be useful for other drug/anionic polymer systems.

ACKNOWLEDGEMENTS

The authors would like to thank Sahand University of Technology Laboratories for their valuable support in the experimental part.

AUTHOR CONTRIBUTION

Maryam Maghsoodi designed and supervised the study plan and wrote the manuscript. Saeideh Mollaie Astemal performed all the experiments. Ali Nokhodchi helped in editing the manuscript. Hossein Kiaie conducted a formal analysis. Ali Baradar Khoshfetrat helped supervise the project. Fatemeh Talebi performed the permeation studies.

FUNDING

No funding to declare.

DECLARATIONS

Conflict of Interest The authors declare no competing interests.

REFERENCES

1. Babu NJ, Nangia A. Solubility advantage of amorphous drugs and pharmaceutical cocrystals. Cryst Growth Des. 2011;11:2662–79.
2. Williams HD, Trevaskis NL, Charman SA, Shanker M, Charman WN, Pouton CW, et al. Strategies to address low drug solubility in discovery and development. Pharmacol Rev. 2013;65:315–499.
3. Brouwers J, Brewster ME, Augustijns P. Supersaturating drug delivery systems: the answer to solubility-limited oral bioavailability? J Pharm Sci. 2009;98:2549–72.
4. Raina SA, Zhang GGZ, Alonzo DE, Wu J, Zhu D, Catron ND, Gao Y, Taylor LS. Enhancements and limits in drug membrane transport using supersaturated solutions of poorly water soluble drugs. J Pharm Sci. 2014;103:2736–48.
5. Kojima T, Higashi K, Suzuki T, Tomono K, Moribe K, Yamamoto K. Stabilization of a supersaturated solution of mefenamic acid from a solid dispersion with Eudragit® EPO. Pharm Res. 2012;29:2777–91.
6. Morgen M, Bloom C, Beyerinck R, Bello A, Song W, Wilkinson K, Steenwyk R, Shamblin S. Polymeric nanoparticles for increased oral bioavailability and rapid absorption using celecoxib as a model of a low-solubility, high-permeability drug. Pharm Res. 2012;29:427–40.
7. Dahan A, Miller JM. The solubility–permeability interplay and its implications in formulation design and development for poorly soluble drugs. AAPS J. 2012;14:244–51.
8. Miller DA, DiNunzio JC, Yang W, McGinity JW, Williams RO. Targeted intestinal delivery of supersaturated itraconazole for improved oral absorption. Pharm Res. 2008;25:1450–9.
9. Wu CY, Benet LZ. Predicting drug disposition *via* application of BCS: transport/absorption/elimination interplay and development of a biopharmaceutics drug disposition classification system. Pharm Res. 2005;22:11–23.
10. Hsieh YL, Ilevbare GA, Van Eerdenbrugh B, Box KJ, Sanchez-Felix MV, Taylor LS. pH-induced precipitation behavior of weakly basic compounds: determination of extent and duration of supersaturation using potentiometric titration and correlation to solid state properties. Pharm Res. 2012;29:2738–53.
11. Stillhart C, Kuentz M. Trends in the assessment of drug supersaturation and precipitation in vitro using lipid-based delivery systems. J Pharm Sci. 2016;105:2468–76.
12. Miller JM, Beig A, Carr RA, Spence JK, Dahan A. A win-win solution in oral delivery of lipophilic drugs: supersaturation *via* amorphous solid dispersions increases apparent solubility without sacrifice of intestinal membrane permeability. Mol Pharm. 2012;9:2009–16.
13. Takano R, Takata N, Saito R, Furumoto K, Higo S, Hayashi Y, Machida M, Aso Y, Yamashita S. Quantitative analysis of the effect of supersaturation on in vivo drug absorption. Mol Pharm. 2010;7:1431–40.
14. Miller DA, DiNunzio JC, Yang W, McGinity JW, Williams RO. Enhanced in vivo absorption of itraconazole via stabilization of supersaturation following acidic-to-neutral pH transition. Drug Dev Ind Pharm. 2008;34:890–902.
15. Curatolo W, Nightingale JA, Herbig SM. Utility of hydroxypropylmethylcellulose acetate succinate (HPMCAS) for initiation and maintenance of drug supersaturation in the GI milieu. Pharm Res. 2009;26:1419–31.
16. Alhnan MA, Cosi D, Murdan S, Basit AW. Inhibiting the gastric burst release of drugs from enteric microparticles: the influence of drug molecular mass and solubility. J Pharm Sci. 2010;99:4576–83.
17. Järvinen T, Järvinen K, Schwarting N, Stella VJ. β-Cyclodextrin derivatives, SBE4-β-CD and HP–β-CD, increase the oral bioavailability of cinnarizine in beagle dogs. J Pharm Sci. 1995;84:295–9.
18. Gao P, Akrami A, Alvarez F, Hu J, Li L, Ma C, Surapaneni S. Characterization and optimization of AMG 517 supersaturatable self-emulsifying drug delivery system (S-SEDDS) for improved oral absorption. J Pharm Sci. 2009;98:516–28.
19. Raghavan SL, Kiepfer B, Davis AF, Kazarian SG, Hadgraft J. Membrane transport of hydrocortisone acetate from supersaturated solutions: the role of polymers. Int J Pharm. 2001;221:95–105.
20. Raghavan SL, Trividic A, Davis AF, Hadgraft J. Effect of cellulose polymers on supersaturation and in vitro membrane

transport of hydrocortisone acetate. Int J Pharm. 2000;193:231–7.
21. Maghsoodi M, Nokhodchi A, Oskuei MA, Heidari S. Formulation of cinnarizine for stabilization of its physiologically generated supersaturation. AAPS PharmSciTech. 2019;20:139.
22. Artursson P, Palm K, Luthman K. Caco-2 monolayers in experimental and theoretical predictions of drug transport. Adv Drug Deliv Rev. 2001;46:27–43.
23. Friesen DT, Shanker R, Crew M, Smithey DT, Curatolo WJ, Nightingale JA. Hydroxypropyl methylcellulose acetate succinate-based spray-dried dispersions: an overview. Mol Pharm. 2008;5:1003–19.
24. Taylor LS, Zhang GGZ. Physical chemistry of supersaturated solutions and implications for oral absorption. Adv Drug Deliv Rev. 2016;101:122–42.
25. Baghel S, Cathcart H, O'Reilly NJ. Understanding the generation and maintenance of supersaturation during the dissolution of amorphous solid dispersions using modulated DSC and 1H NMR. Int J Pharm. 2018;536:414–25.
26. Frank KJ, Westedt U, Rosenblatt KM, Hölig P, Rosenberg J, Mägerlein M, Fricker G, Brandl M. What is the mechanism behind increased permeation rate of a poorly soluble drug from aqueous dispersions of an amorphous solid dispersion? J Pharm Sci. 2014;103:1779–86.
27. Bevernage J, Brouwers J, Annaert P, Augustijns P. Drug precipitation–permeation interplay: supersaturation in an absorptive environment. Eur J Pharm Biopharm. 2012;82:424–8.
28. Kataoka M, Takeyama S, Minami K, Higashino H, Kakimi K, Fujii Y, Takahashi M, Yamashita S. In vitro assessment of supersaturation/precipitation and biological membrane permeation of poorly water-soluble drugs: a case study with albendazole and ketoconazole. J Pharm Sci. 2019;108:2580–7.
29. Alhayali A, Selo MA, Ehrhardt C, Velaga S. Investigation of supersaturation and in vitro permeation of the poorly water soluble drug ezetimibe. Eur J Pharm Sci. 2018;117:147–53.
30. Gu CH, Rao D, Gandhi RB, Hilden J, Raghavan K. Using a novel multicompartment dissolution system to predict the effect of gastric pH on the oral absorption of weak bases with poor intrinsic solubility. J Pharm Sci. 2005;94:199–208.
31. Alonzo DE, Raina S, Zhou D, Gao Y, Zhang GGZ, Taylor LS. Characterizing the impact of hydroxypropylmethyl cellulose on the growth and nucleation kinetics of felodipine from supersaturated solutions. Cryst Growth Des. 2012;12:1538–47.
32. Ilevbare GA, Liu H, Edgar KJ, Taylor LS. Effect of binary additive combinations on solution crystal growth of the poorly water-soluble drug, ritonavir. Cryst Growth Des. 2012;12:6050–60.
33. Kiew TY, Cheow WS, Hadinoto K. Preserving the supersaturation generation capability of amorphous drug-polysaccharide nanoparticle complex after freeze drying. Int J Pharm. 2015;484:115–23.
34. Xie T, Taylor LS. Dissolution performance of high drug loading celecoxib amorphous solid dispersions formulated with polymer combinations. Pharm Res. 2016;33:739–50.
35. Yokoi Y, Yonemochi E, Terada K. Effects of sugar ester and hydroxypropyl methylcellulose on the physicochemical stability of amorphous cefditoren pivoxil in aqueous suspension. Int J Pharm. 2005;290:91–9.
36. Ilevbare GA, Liu H, Edgar KJ, Taylor LS. Understanding polymer properties important for crystal growth inhibition-impact of chemically diverse polymers on solution crystal growth of ritonavir. Cryst Growth Des. 2012;12:3133–43.
37. Ilevbare GA, Liu H, Edgar KJ, Taylor LS. Maintaining supersaturation in aqueous drug solutions: impact of different polymers on induction times. Cryst Growth Des. 2013;13:740–51.
38. Miladi K, Ibraheem D, Iqbal M, Sfar S, Fessi H, Elaissari A. Particles from preformed polymers as carriers for drug delivery. EXCLI J. 2014;13:28–57.
39. Thakral S, Thakral NK, Majumdar DK. Eudragit®: a technology evaluation. Expert Opin Drug Deliv. 2013;10:131–49.
40. Ilevbare GA, Liu H, Edgar KJ, Taylor LS. Inhibition of solution crystal growth of ritonavir by cellulose polymers–factors influencing polymer effectiveness. Cryst Eng Comm. 2012;14:6503–14.
41. Ilevbare GA, Liu H, Edgar KJ, Taylor LS. Impact of polymers on crystal growth rate of structurally diverse compounds from aqueous solution. Mol Pharm. 2013;10:2381–93.
42. Amis EJ, Hu N, Seery TAP, Hogen-Esch TE, Yassini M, Hwang F. Associating polymers containing fluorocarbon hydrophobic units. Adv Chem. 1996;248.
43. Shi NQ, Jin Y, Zhang Y, Che XX, Xiao X, Cui GH, Chen YZ, Feng B, Li ZQ, Qi XR. The influence of cellulosic polymer's variables on dissolution/solubility of amorphous felodipine and crystallization inhibition from a supersaturated state. AAPS PharmSciTech. 2018;20:12.
44. Li Z, Johnson LM, Ricarte RG, Yao LJ, Hillmyer MA, Bates FS, Lodge TP. Enhanced performance of blended polymer excipients in delivering a hydrophobic drug through the synergistic action of micelles and HPMCAS. Langmuir. 2017;33:2837–48.
45. Abu-Diak OA, Jones DS, Andrews GP. Understanding the performance of melt-extruded poly(ethylene oxide)–bicalutamide solid dispersions: characterisation of microstructural properties using thermal, spectroscopic and drug release methods. J Pharm Sci. 2012;101:200–13.
46. Wang S, Liu C, Chen Y, Zhu AD, Qian F. Aggregation of hydroxypropyl methylcellulose acetate succinate under its dissolving pH and the impact on drug supersaturation. Mol Pharm. 2018;15:4643–53.
47. Serajuddin AT. Salt formation to improve drug solubility. Adv Drug Deliv Rev. 2007;59:603–16.
48. Ozaki S, Minamisono T, Yamashita T, Kato T, Kushida I. Supersaturation–nucleation behavior of poorly soluble drugs and its impact on the oral absorption of drugs in thermodynamically high-energy forms. J Pharm Sci. 2012;101:214–22.
49. Turnbull D, Fisher JC. Rate of nucleation in condensed systems. J Chem Phys. 1949;17:71–3.
50. Carlert S, Pålsson A, Hanisch G, von Corswant C, Nilsson C, Lindfors L, Lennernäs H, Abrahamsson B. Predicting intestinal precipitation—a case example for a basic BCS Class II Drug. Pharm Res. 2010;27:2119–30.
51. Lang B, Liu S, McGinity JW, Williams RO. Effect of hydrophilic additives on the dissolution and pharmacokinetic properties of itraconazole-enteric polymer hot-melt extruded amorphous solid dispersions. Drug Dev Ind Pharm. 2016;42:429–45.
52. Ilevbare GA, Taylor LS. Liquid–liquid phase separation in highly supersaturated aqueous solutions of poorly water-soluble drugs: implications for solubility enhancing formulations. Cryst Growth Des. 2013;13:1497–509.
53. Murdande SB, Pikal MJ, Shanker RM, Bogner RH. Solubility advantage of amorphous pharmaceuticals: I. A thermodynamic analysis. J Pharm Sci. 2010;99:1254–64.
54. Jackson MJ, Kestur US, Hussain MA, Taylor LS. Dissolution of danazol amorphous solid dispersions: supersaturation and phase behavior as a function of drug loading and polymer type. Mol Pharm. 2016;13:223–31.
55. Indulkar AS, Gao Y, Raina SA, Zhang GG, Taylor LS. Exploiting the phenomenon of liquid-liquid phase separation for enhanced and sustained membrane transport of a poorly water-soluble drug. Mol Pharm. 2016;13:2059–69.
56. Indulkar AS, Box KJ, Taylor R, Ruiz R, Taylor LS. pH-dependent liquid-liquid phase separation of highly supersaturated solutions of weakly basic drugs. Mol Pharm. 2015;12:2365–77.
57. Van Eerdenbrugh B, Raina S, Hsieh YL, Augustijns P, Taylor LS. Classification of the crystallization behavior of amorphous active pharmaceutical ingredients in aqueous environments. Pharm Res. 2014;31:969–82.
58. Raina SA, Van Eerdenbrugh B, Alonzo DE, Mo H, Zhang GGZ, Gao Y, et al. Trends in the precipitation and crystallization behavior of supersaturated aqueous solutions of poorly water-soluble drugs assessed using synchrotron radiation. J Pharm Sci. 2015;104:1981–92.
59. Haress NG. Chapter One-Cinnarizine: comprehensive profile. in: H.G. Brittain (Ed.). Profiles of drug substances, excipients and related methodology. Academic Press. 2015, pp. 1-41.
60. Raghavan SL, Trividic A, Davis AF, Hadgraft J. Crystallization of hydrocortisone acetate: influence of polymers. Int J Pharm. 2001;212:213–21.

61. Gao P, Guyton ME, Huang T, Bauer JM, Stefanski KJ, Lu Q. Enhanced oral bioavailability of a poorly water soluble drug PNU-91325 by supersaturatable formulations. Drug Dev Ind Pharm. 2004;30:221–9.
62. Cilurzo F, Minghetti P, Selmin F, Casiraghi A, Montanari L. Polymethacrylate salts as new low-swellable mucoadhesive materials. J Control Release. 2003;88:43–53.
63. Yoo S, Krill SL, Wang Z, Telang C. Miscibility/stability considerations in binary solid dispersion systems composed of functional excipients towards the design of multi-component amorphous systems. J Pharm Sci. 2009;98:4711–23.
64. Kanzer J, Tho I, Flaten GE, Mägerlein M, Hölig P, Fricker G, Brandl M. In-vitro permeability screening of melt extrudate formulations containing poorly water-soluble drug compounds using the phospholipid vesicle-based barrier. J Pharm Pharmacol. 2010;62:1591–8.
65. Hubatsch I, Ragnarsson EGE, Artursson P. Determination of drug permeability and prediction of drug absorption in Caco-2 monolayers. Nat Protoc. 2007;2:2111–9.
66. Bevernage J, Brouwers J, Annaert P, Augustijn P. Drug precipitation–permeation interplay: supersaturation in an absorptive environment. Eur J Pharm Biopharm. 2012;82:424–8.
67. Frank KJ, Rosenblatt KM, Westedt U, Hölig P, Rosenberg J, Mägerlein M, Fricker G, Brandl M. Amorphous solid dispersion enhances permeation of poorly soluble ABT-102: true supersaturation vs. apparent solubility enhancement. Int J Pharm. 2012;437:288–93.
68. Saha P, Kou JH. Effect of solubilizing excipients on permeation of poorly water-soluble compounds across Caco-2 cell monolayers. Eur J Pharm Biopharm. 2000;50:403–11.